University of Bristol - Explore Bristol Research
General rights

A robust and reliability-based aeroelastic tailoring framework for composite aircraft wings

Muhammad F. Othman[a,b,*], Gustavo H.C. Silva[c], Pedro H. Cabral[c], Alex P. Prado[c], Alberto Pirrera[a], Jonathan E. Cooper[a]

[a] *Bristol Composites Institute (ACCIS), Department of Aerospace Engineering, University of Bristol, Queen's Building, University Walk, Bristol BS8 1TR, UK*
[b] *School of Mechanical Engineering, Universiti Sains Malaysia, Engineering Campus, 14300 Nibong Tebal, Penang, Malaysia*
[c] *Embraer S.A., São José dos Campos, São Paulo, 12227-901, Brazil*

ABSTRACT

This paper presents a multi-level aeroelastic tailoring framework for the optimisation of composite aircraft wings. The framework is capable of structural sizing and produces detailed composite ply configurations through robust and reliability-based design optimisation, and is demonstrated on a representative regional jet airliner finite element wing box model. The optimisation procedure is divided into two levels. The first level optimises the wing structure for minimum weight subject to multiple constraints including strain, buckling, aeroelastic stability and gust response. These first level solutions are then fed into the second level to be further optimised for robustness or reliability by considering uncertainties in material properties at ply level. Both the principles of robust and reliability-based design optimisation can also be used in combination to ensure a balance between the robustness and reliability of the structural performance. In order to keep computations to an acceptable cost, the second level optimisation employs the Polynomial Chaos Expansion method to approximate the effect of probabilistic uncertainty on structural performance. In comparison to the original benchmark wing, the framework produces an overall weight reduction of 32.1%, despite a 1.5% increase from the first to the second level optimisation that accounts for stochastic design variations.

1. Introduction

The design of aeroelastically-tailored aircraft structures—intended for maximum performance and minimum weight—remains a challenging multidisciplinary optimisation problem. Although the possibility, and the consequent benefits, of aeroelastic tailoring through composite materials have been around since the early 1980s, most of the designs proposed by the research community have been based on the so-called 'black metal' approach, which does not exploit anisotropy fully. This somewhat conservative attitude is at odds with the elastic tailoring capabilities offered by composite materials, which, by allowing bending-torsion stiffness coupling terms to be modified, lend themselves to innovative design solutions for improved aeroelastic performance.

A significant amount of work can be found in the literature concerning the design and optimisation of aeroelastically-tailored composite wing structures. Typically, research has focused on optimising wings for minimum structural weight, subject to multiple constraints

including stress [1,2], strain [3], buckling [4], aeroelastic response [1,5–7] and gust response [8]. All of these studies report of modifications of the wing's composite panels to design for passively coupled bending-torsional deformations.

Concurrently, considerable efforts have been devoted to develop the aeroelastic tailoring design process to improve both its accuracy and computational efficiency. In particular, in order to circumvent the computational cost associated with detailed, high fidelity wing representations, some authors adopted simplified models, while others recurred to efficient optimisation techniques. Examples of the former case include: Refs. [?,9–12], which approximated composite lifting surfaces as cantilever plates and optimised for aeroelastic stability, neglecting the effects on structural weight; and Refs. [3,7,13–16], which used wing-box models, including skins, spar and ribs, in order to obtain a more accurate structural and aeroelastic performance characterisation. Examples of the latter case, instead, include the work by Kuzmina and Guo [2,3] and Gasbarri et al. [17] that employed multi-objective or hybrid optimisation procedures. In their approach, the

optimisations are divided into stages to address multiple objectives or constraints, which leads to enhanced computational efficiency.

Traditionally, aircraft wing structures are designed using deterministic approaches for minimum structural weight, while satisfying multiple constraints for performance and certification. Designers, however, are aware that deterministic optimisations, being unable to account for probabilistic uncertainties, may lead to unreliable or unrealistic designs. There are two types of uncertainty that can be classified as *'epistemic'* and *'aleatory'*. As described by Melchers [18], epistemic uncertainty is a type of uncertainty arise from limitation of knowledge which is often due to lack of understanding about the physics and human errors. Aleatory uncertainty is an irreducible uncertainty which is inherent to the system or model. When dealing with aircraft design, uncertainties may arise from human errors, geometric and material properties, and from manufacturing processes. If one were to design for reliability and robustness, these uncertainties should be quantified accurately. Hence, the growing interest in improving or replacing deterministic optimisation procedures for robust and reliability-based structural design methods.

Including parameter uncertainty in design optimisation implies solving the problem with sampling or quantification methods such as Monte Carlo Simulation (MCS) [8,19], Polynomial Chaos Expansion (PCE) [12,16,20,21] or Stochastic Collocation [22]. MCS is the most common and straightforward technique to quantify uncertainty in a model; however, great computational efforts are required to produce meaningful results. The effectiveness of PCE over MCS has been reported in Refs. [12,20] in relation to plate wing models for aeroelastic analyses, where it was shown that using a sampling methods such as PCE reduces the number of runs required to fully characterise the model's uncertainty, in comparison to MCS. A finding of obvious potential benefit for uncertainty-based design optimisations.

In the context of aeroelastic design of composite structures, aleatoric uncertainty arises from a number of sources, including structural geometry, errors in aerodynamic predictions, variability in material properties such as material non-homogeneity, fibre misalignment, waviness, wrinkling and defects, as well as manufacturing tolerances and thickness variations. These uncertainties are to be quantified accurately in order to produce realistic designs accounting for robustness and reliability. The literature reports two main methodologies for uncertainty-based design optimisation: 1) Reliability-Based Design Optimisation (RBDO) [12,23–25] and 2) Robust Design Optimisation (RDO) [24,26]. RBDO aims at optimising a design whilst having a particular risk or target reliability/performance as a constraint. RDO seeks optimal designs about a mean response value thereby maximising robustness via minimisation of the sensitivity to random parameter variations [24]. A mixed approach, which employs features of both RDO and RBDO is thought to be a more effective means to search for robust optima that also satisfy reliability constraints. Paiva et al. [24] used a mixed RDO-RBDO approach for the preliminary design of aircraft wings. Their multidisciplinary approach employs a Kriging surrogate model to account for uncertainty in parameters of flight condition.

The application of probabilistic optimisation approaches such as RBDO and RDO for the aeroelastic tailoring of composite structures has been reported by several authors [12,23,25]. Scarth et al. [12] and Manan et al. [23] used simplified analytical models for aeroelastic stability with uncertainty arising from composite material properties. These works employ a PCE model for uncertainty evaluation, together with a singly-constrained RBDO approach, to obtain a reliable design for maximum instability speed. In contrast, the work presented in this paper employs a detailed finite element wing box model, together with a PCE surrogate model for uncertainty quantification, for a multi-constrained aeroelastic tailoring optimisation problem. In addition, robust and reliability-based design methods are used in combination within a multi-level optimisation framework.
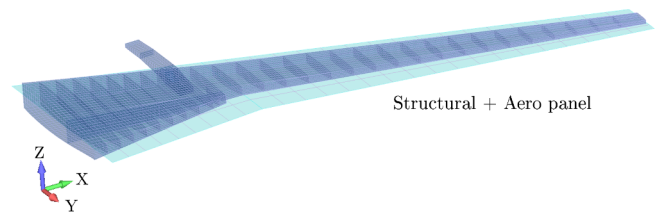

Fig. 1. Architecture, Finite Element model and aerodynamic panelling of the benchmark composite wing.

This paper introduces a multi-level aeroelastic tailoring optimisation approach to determine minimum structural wing weight, subject to multiple structural and aeroelastic constraints. The optimisation procedure is divided into two levels: a deterministic optimisation and a combined implementation of robust and reliability-based design optimisations (RRBDO). Composite material properties and ply thickness variations are chosen as the parameters carrying uncertainty, with different levels of variation. A comparison between the RDO, RBDO and RRBDO approaches for aeroelastic tailoring is presented. It is found that the proposed multi-level aeroelastic approach enables the designer to rapidly evaluate minimum weight solutions for composite wings and also account for considerations of robustness and design reliability.

2. Model definition and analysis methods

A detailed Finite Element (FE) model for the high aspect ratio wing box of a reference regional jet airliner is used for the analyses presented in this paper. The model is shown in Fig. 1. Planform and wing box geometry are depicted in Fig. 2 with dimensions normalised to the wing semi-span. The structure is modelled in MSC PATRAN 2013 using CQUAD4 shell elements for the spars, ribs and skins and CBAR beam elements for the stringers. The model comprises three spars, 30 ribs and 14 stringers. All parts of the primary structure are made of intermediate modulus carbon/epoxy composite (Hexcel 8552 IM7 [27]), with material properties listed in Table 1.

A total of 25471 elements and 16453 nodes are used in the structural mesh to ensure converged results. The aerodynamic panelling, also shown in Fig. 1, is divided into two sections, with the outer wing having a higher mesh density compared to the inner wing. The model's aerodynamic grid and structural mesh are coupled using a surface spline to transfer loads from the aerodynamic grid points to the FE nodes.

For dynamic and aeroelastic analyses, engine and fuel weight are modelled as concentrated masses, with locations as shown in Fig. 2(a). The fuel mass is distributed spanwise along the tank centroid line, with point masses positioned between each spar-rib bay.

Only skin and spar sections are included in the optimisation procedures, where a total of 41 panels is created, with 11 panels for top and bottom skins, eight panels for spar 1 and 2, and three panels for spar 3, as shown in Fig. 2(b). As mentioned in the introduction, the wing model is optimised for minimum weight with consideration of robustness and reliability, when subject to multiple constraints including strain, buckling, aeroelastic stability and extreme gust loads. Lamination parameters and laminate thickness are chosen as design variables and translated into stiffness components to be input into the FE model.

2.1. Lamination parameters

Lamination parameters provide a compact and computationally inexpensive mathematical representation for composite lay-ups and are, therefore, adopted in this paper. In the most general case, by using
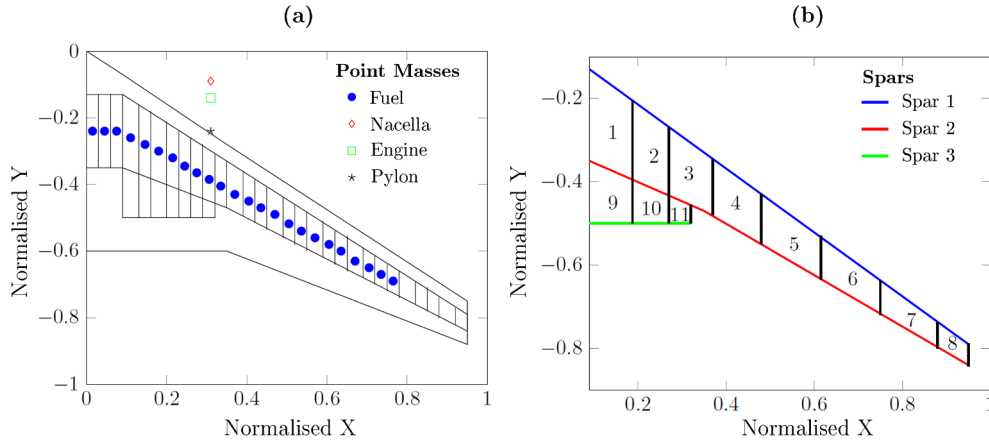
Fig. 2. Wing geometry: (a) General dimension and location of *'point masses'*; (b) Panel partitions for skin and spar sections.

Table 1
Composite material properties (Hexcel 8552 IM7) [27].

Property	Value
E_1 (GPa)	148.0
E_2 (GPa)	10.3
G_{12} (GPa)	5.90
υ_{12}	0.27
Density, ρ (kg m^{-3})	1580
Ply thickness, t_{ply} (mm)	0.183

the so-called material invariants, 12 lamination parameters and the laminate thickness are sufficient to define the full set of stiffness coefficients describing a composite stack [28]. This compact definition greatly reduces the number of unknown variables required to specify a stacking sequence. In addition, lamination parameters are continuous variables and therefore lend themselves to efficient gradient-based optimisations. The mapping between lamination parameters and lay-ups, however, is not bi-objective. Not all sets of lamination parameters correspond to feasible stacking sequences. Additionally, a point in lamination parameter space may map onto multiple stacking sequences. For these reasons, the aforementioned gradient-based optimisations are usually constrained to operate within feasibility regions defined by inequalities relating the lamination parameters. Stacking sequences are then retrieved from lamination parameters by solution of an additional optimisation problem. An example is given by Kameyama and Fukunaga [29] that utilised lamination parameters as intermediate design variables for the minimum weight optimisation of composite plate wings subject to flutter and divergence constraints.

According to Classical Laminate Theory (CLT) [30], the relation between generalised internal forces and generalised deformations for symmetric laminates is given by

$$\begin{Bmatrix} N \\ M \end{Bmatrix} = \begin{bmatrix} A & 0 \\ 0 & D \end{bmatrix} \begin{Bmatrix} \epsilon \\ \kappa \end{Bmatrix}, \tag{1}$$

where A and D represent the laminate's stretching and bending stiffnesses, respectively, $N = \{N_x, N_y, N_{xy}\}^T$ and $M = \{M_x, M_y, M_{xy}\}^T$ are resultant forces and moments per unit length, and $\epsilon = \{\epsilon_x, \epsilon_y, \epsilon_{xy}\}^T$ and $\kappa = \{\kappa_x, \kappa_y, \kappa_{xy}\}^T$ are in-plane stretching terms, and bending and twist curvatures. The stiffness components, A_{ij} and D_{ij}, can be calculated from the stiffness invariants, $\{U\}$, and the in-plane and out-of-plane lamination parameters, ξ_k^A and ξ_k^D (where $k = 1, 2, 3, 4$), by means of the following equations:

$$\begin{Bmatrix} A_{11} \\ A_{12} \\ A_{22} \\ A_{66} \\ A_{16} \\ A_{26} \end{Bmatrix} = t \begin{bmatrix} 1 & \xi_1^A & \xi_2^A & 0 & 0 \\ 0 & 0 & -\xi_2^A & 1 & 0 \\ 1 & -\xi_1^A & \xi_2^A & 0 & 0 \\ 0 & 0 & -\xi_2^A & 0 & 1 \\ 0 & \frac{\xi_3^A}{2} & \xi_4^A & 0 & 0 \\ 0 & \frac{\xi_3^A}{2} & -\xi_4^A & 0 & 0 \end{bmatrix} \begin{Bmatrix} U_1 \\ U_2 \\ U_3 \\ U_4 \\ U_5 \end{Bmatrix} \tag{2}$$

and

$$\begin{Bmatrix} D_{11} \\ D_{12} \\ D_{22} \\ D_{66} \\ D_{16} \\ D_{26} \end{Bmatrix} = \frac{t^3}{12} \begin{bmatrix} 1 & \xi_1^D & \xi_2^D & 0 & 0 \\ 0 & 0 & -\xi_2^D & 1 & 0 \\ 1 & -\xi_1^D & \xi_2^D & 0 & 0 \\ 0 & 0 & -\xi_2^D & 0 & 1 \\ 0 & \frac{\xi_3^D}{2} & \xi_4^D & 0 & 0 \\ 0 & \frac{\xi_3^D}{2} & -\xi_4^D & 0 & 0 \end{bmatrix} \begin{Bmatrix} U_1 \\ U_2 \\ U_3 \\ U_4 \\ U_5 \end{Bmatrix}, \tag{3}$$

where t is the thickness of the laminate.

By defining the non-dimensional through-thickness coordinate , the lamination parameters can be expressed in terms of ply orientation θ as

$$\xi_{[1,2,3,4]}^A = \frac{1}{2} \int_{-1}^1 \{\cos2\theta(u), \cos4\theta(u), \sin2\theta(u), \sin4\theta(u)\} du \tag{4}$$

and

$$\xi_{[1,2,3,4]}^D = \frac{3}{2} \int_{-1}^1 \{\cos2\theta(u), \cos4\theta(u), \sin2\theta(u), \sin4\theta(u)\} u^2 \, du. \tag{5}$$

Bloomfield et al. [28] provide a comprehensive overview on the feasible regions of lamination parameters. In this work, we use the inequalities derived by Fukunaga and Sekine [31], which describe the feasible regions of the four in-plane and out-of-plane lamination parameters. These are

$$-1 \leqslant (\xi_k^j) \leqslant 1, \tag{6a}$$

$$(\xi_1^j)^2 + (\xi_3^j)^2 \leqslant 1, \tag{6b}$$

$$2(1 + \xi_2^j)(\xi_3^j)^2 - 4\xi_1^j\xi_3^j\xi_4^j + (\xi_4^j)^2 - (\xi_2^j - 2(\xi_1^j)^2 + 1)(1 - \xi_2^j) \leqslant 0, \tag{6c}$$

where $k = 1, 2, 3, 4$ and $j = A, D$.

Current practice in the design and optimisation of composite laminates is to restrict the design space to balanced and symmetric lay-ups, to enable feasible manufacture. One of the reasons is that non-symmetric laminates tend to warp upon cool down from curing temperature, and unbalanced laminates have shear-extension coupling. For

balanced laminates, the lamination parameters ξ_3^j and ξ_4^j vanish and hence, the bend-twist coupling stiffness, D_{16} and D_{26}, are zero. This effect reduces the influence of anisotropy (bend-twist coupling) on the response of composite structures [32], thereby reducing the design spaces for aeroelastic tailoring. In order to avoid this limitation, non-balanced, symmetric laminates are considered in this work. This decision results in nine design variables for each composite panel in the wing box model (eight lamination parameters plus one laminate thickness), giving a cumulative total of 369 design variables for each level of optimisation.

2.2. Aeroelastic analysis

The aeroelastic stability of the wing box is assessed using MSC NASTRAN's SOL 145, which employs the frequency matching *'p-k'* method to predict the flutter speed, V_f. Further details can be found in [33]. Structural frequencies, as well as their modal amplitudes and damping, are obtained from the analysis as functions of air speed. The flutter speed for each mode is found from the value at which the damping become negative. A total of 12 modes are considered in the flutter analysis to allow for an adequate representation of the aeroelastic behaviour.

2.3. Gust response

The optimisation of composite wings for gust load alleviation has been explored by various researchers [3,8,34,35]. As specified by aeronautical authorities (CS-25 [36]), the dynamic gust load conditions for an aircraft consists of discrete gust and continuous turbulence (or continuous gust). For discrete gust load, the gust velocity varies in deterministic manner which is represented using *'1-cosine'* gust profile. For continuous gust load, the gust velocity is assumed to vary in a random manner. The deterministic method employs 'worst-case' atmospheric gust approach where there is an idealised 'discrete' event that the aircraft encounters during flight time. Herein, the deterministic method is used to analyse the wing's response in terms of root bending moment (RBM) due to worst-case gust scenario [8,20]. The variation in air velocity, in the direction normal to the aircraft path, is shown in Fig. 3. The expression governing the *'1-cosine'* gust is given by

$$V_g(t) = \frac{V_{g0}}{2}\left(1-\cos\frac{2\pi V}{L_g}t\right),\tag{7}$$

where V_{g0} is the peak or design gust velocity, L_g is the gust length and V is the flight speed. In this work, the gust length is chosen to vary from 18 m to 216 m. The design gust velocity and flight speed are set to 20 ms^{-1} and 253 ms^{-1}, respectively. MSC NASTRAN's SOL 146 is used to evaluate the wing box dynamic aeroelastic response to discrete gusts.
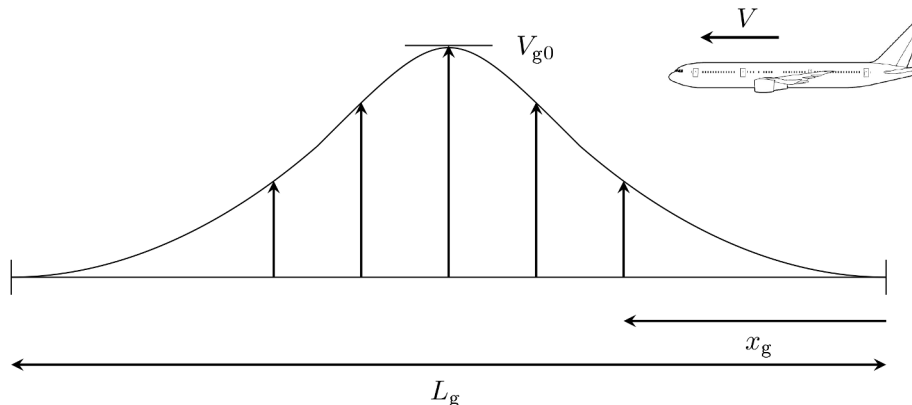
3. Multi-level aeroelastic tailoring

A multi-level optimisation method is proposed for the aeroelastic tailoring of the composite wing box of a reference regional jet airliner and the various optimisation methodologies, algorithms and strategies are detailed in this section.

The objective of the optimisation process is to minimise structural weight, subject to multiple constraints, including strength and aeroelastic stability. Thickness and lamination parameters of the wing box composite panels are used as design variables. The design's robustness and reliability, when considering stochastic variations of composite ply material properties and thickness, are also assessed.

The optimisation framework comprises two levels, as illustrated in Fig. 4. MATLAB's implementation of the Particle Swarm Optimisation (PSO) algorithm and MSC NASTRAN are used to solve the optimisation problem. PSO is a heuristic search method based on simple analogues of collaborative behaviour and swarming in biological populations [37]. Similar to a Genetic Algorithm (GA), PSOs perform population-based searches that depend on exchanges of information between individuals for search progression. PSO is reported to be computationally more efficient than GAs, because the algorithm requires fewer function evaluations [38].

The PCE, as presented by [23,12], is used as a non-sampling-based method to quantify model uncertainty and create surrogate models for robust and reliability-based design optimisation. The PCE method is developed such that the model is assumed to be a black-box with unknown inner structures. The method is straightforward as the model response of random value y is represented by random vector x rather than the distribution density function.

In the first level optimisation, the wing structure is subjected to a static manoeuvre load and optimised for minimum weight with strain, buckling, flutter and gust response constraints. The load distribution due to the aerodynamic loading is obtained from a trim analysis performed with MSC NASTRAN's SOL 144. The static manoeuvre load case is run at a Mach 0.82, cruise altitude 10, 000 m and acceleration 2.5 g. Fuel load is included to provide a realistic representation of the wing model. A weighted cost function is used to account for the influence of multiple constraints.

Results from the first level are fed to the second level to optimise the design further for robustness and reliability. The effect of uncertainties on flutter response is considered in terms of probability (of failure) density functions (PDF). To keep computational time to acceptable levels, the effect of uncertainties on other first level constraints is not quantified explicitly. However, for consistency, first level responses are imposed as design constraints in the second level.
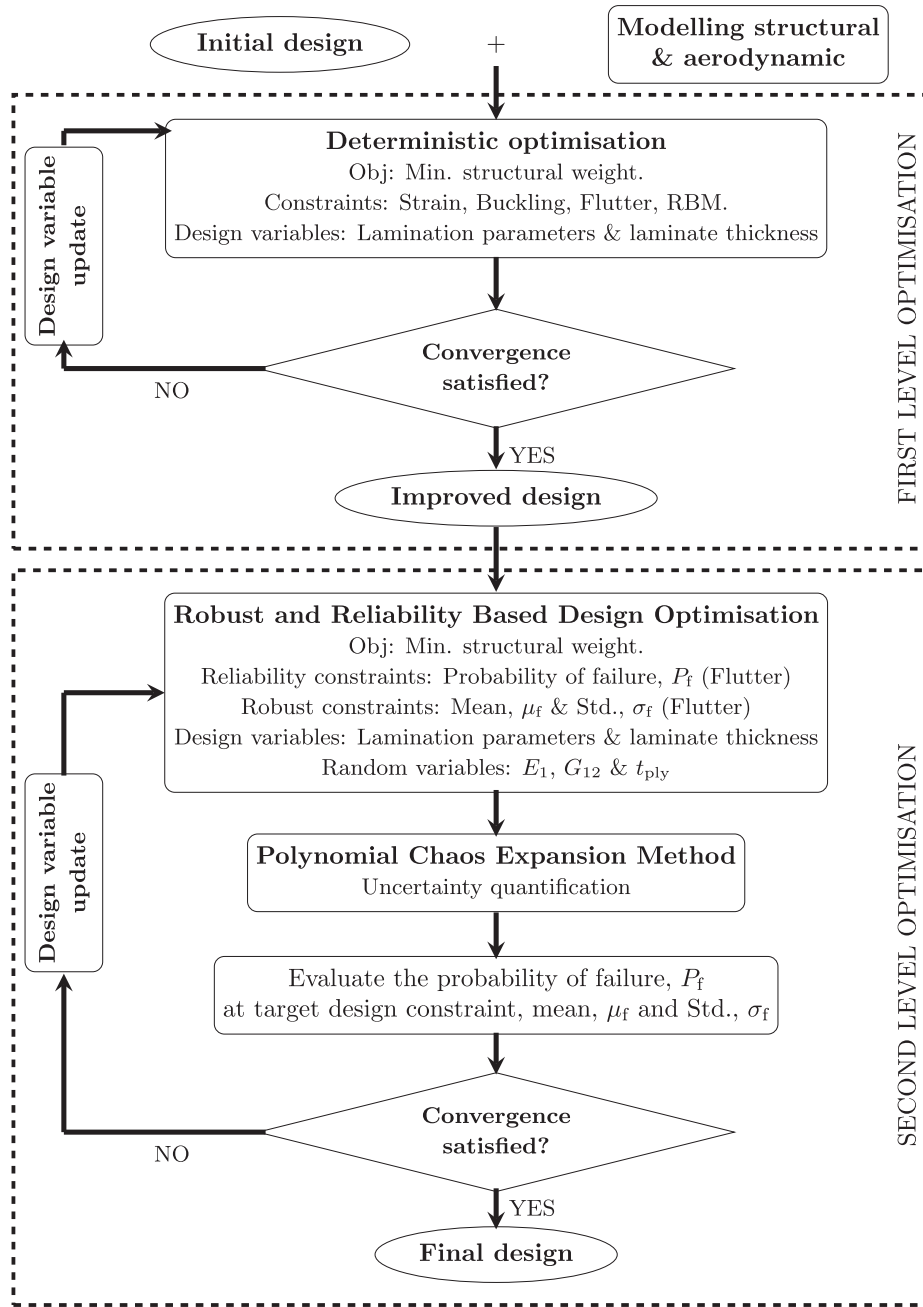

Fig. 3. *'1-cosine'.* discrete gust representation (x_g is the flight travel distance).

Fig. 4. The multi-level optimisation approach.

3.1. First level: Deterministic optimisation

The first level optimisation problem is formulated as follows:

$$\underset{\mathbf{x}}{\text{minimize}} \; f_{\text{obj}}(W(\mathbf{x}), f_{1,\text{cost}}(\mathbf{x})),$$

subject to: Strain Failure Index, $FI(\mathbf{x}) \leqslant 1$ (Max. Strain),

Buckling critical load factor, $\lambda(\mathbf{x}) \geqslant 1$,

Flutter speed, $V_f(\mathbf{x}) \geqslant 1.15V_D$ (V_D = Design dive speed),

Wing Root Bending Moment, $\max(RBM(\mathbf{x}, L_g)) \leqslant$

$\max(RBM_{\text{Benchmark}}(L_g))$,

$\mathbf{x} = [\xi_1^A, ..., \xi_4^A, \xi_1^D, ..., \xi_4^D, t_{\text{panel},1}, ..., t_{\text{panel},41}],$

(8)

where

- **x** is vector containing the design variables.
- λ is the lowest buckling load factor (ten modes are computed to account for mode switching).
- FI is the strain Failure Index defined as

$$FI = \max\left(\frac{\varepsilon_x}{\varepsilon_{x,\text{allowable}}}, \frac{\varepsilon_y}{\varepsilon_{y,\text{allowable}}}, \frac{\varepsilon_{xy}}{\varepsilon_{xy,\text{allowable}}}\right) \leqslant 1,$$

(9)

where $\{\varepsilon\} = \{\varepsilon_x, \varepsilon_y, \varepsilon_{xy}\}^T = \{\epsilon\} + z\{\kappa\}$ are the strain components through the laminate's thickness, z, $\varepsilon_{x,\text{allowable}} = \varepsilon_{y,\text{allowable}} = 7100\mu\,\epsilon$ and $\varepsilon_{xy,\text{allowable}} = 4500\mu\,\epsilon$.
- The flutter speed, V_f, is calculated from a conventional *V-g* plot as per §2.2, assuming Mach 0.82 and flight dive velocity, V_D, at 10,000 m. Since 12 modes are considered, V_f is assumed to be the lowest of 12 values at which the damping factor equals zero.
- For the gust constraint, six different values of L_g as indicated in indicated in §2.3 are used in order to compute the maximum RBM.

Table 2
Mean and standard deviation for the parameters carrying uncertainties.

	E_1 (GPa)	G_{12} (GPa)	t_{ply} (m)
Mean, μ	148.0	5.90	1.83×10^{-4}
Std Dev., σ	14.8	0.59	1.83×10^{-6}

The values are selected within the gust gradient distance range (H) of 9 m to 107 m (gust length is twice of gust gradient distance) as specified by European Aviation Safety Agency (EASA). Six values are sufficient to find the critical response for each load quantity.

Finally, the objective function in Eq. (8) is given as

$$f_{\text{obj}} = \frac{W(\mathbf{x})}{W_{\text{Benchmark}}} + f_{1,\text{cost}}(\mathbf{x}),$$
(10)

where W is the wing structural weight (skins and spars only); $f_{1,\text{cost}}(\mathbf{x})$ is a cost penalty function defined to account for constraint violations as

$$f_{1,\text{cost}} = w_f \times \left| \frac{V_f - V_{f,\text{Design}}}{V_{f,\text{Design}}} \right| + w_g \times \left| \frac{RBM}{RBM_{\text{Benchmark}}} \right| + w_{\text{EIG}} \times \left| \frac{\lambda - \lambda_{\text{Design}}}{\lambda_{\text{Design}}} \right|$$
$$+ w_{\text{FI}} \times \left| \frac{FI - FI_{\text{Design}}}{FI_{\text{Design}}} \right|,$$
(11)

and where

$$w_{\text{constr}} = \{ w_{\text{constr}_i} \in [0, 1]: \sum_{\text{constr}_i} w_{\text{constr}_i} = 1, \ \text{constr}_i \in \{f, g, \text{EIG}, \text{FI}\} \}$$
(12)

is the set of weighting coefficients relative to each of the constraints, and the subscript 'Design' denotes desired or allowable values. The design constraints are included in the objective function in the form of cost penalty function. So that, the trade-off between minimum structural weight and optimum constraints values are accounted towards the improved design solution.

By variation of the weighting coefficients, a Pareto front of optimised solutions is obtained. Following the averaging principle defined in [39], the overall best deterministic design is chosen as the Pareto point minimising the expression ($\Sigma - 5$), where

$$\Sigma = \frac{W}{W_{\text{min}}} + \frac{V_f}{V_{f,\text{max}}} + \frac{RBM}{RBM_{\text{min}}} + \frac{\lambda}{\lambda_{\text{min}}} + \frac{FI}{FI_{\text{max}}},$$
(13)

and where the subscripts min and max indicate the minimum and maximum values obtained for each parameter from all possible weighting combinations.

3.2. Second level: Robust and reliability-based design optimisation

The need for a multi-level optimisation strategy is justified by considerations of computational feasibility. Evaluating full wing box designs, for multiple performance/constraint metrics and by means of finite element models, can be costly and take many minutes per attempted solution. Aiming to quantify the effect of parameter uncertainty on the robustness and reliability of optimised designs, one would have to run a statistically relevant number of stochastic variations for every tentative solution trialled by the optimiser. This requirement makes "all-at-once", single level approaches computationally impractical. A potential alternative to alleviate the computational burden is to recur to metamodels or surrogate models to approximate system behaviour with functions that are quick to interrogate and evaluate. However, training the surrogates to capture a variety of responses to multiple parameters is similarly computationally expensive and impractical.

To overcome these limitations, the approach adopted in this work is to run a deterministic optimisation first and then pass the output to a second level, to account for uncertainty. In the second level, PCE is used to quantify the effect of uncertainties on some responses only, using the optimised values of the remaining ones as design constraints. This approach guarantees that the second level output, i.e. the final optimised design, is robust and reliable in terms of chosen responses, whilst still meeting all of the constraints imposed on and met by the deterministic optimum.

Reliability-Based Design Optimisation and Robust Design Optimisation are the two main methodologies reported in the literature for probabilistic design optimisation [23–26,40]. In this work, aleatory variations in material stiffness and ply thickness are considered. In particular, and unless stated otherwise, longitudinal and shear modulus, E_1 and G_{12}, respectively, are assumed to be random variables with coefficient of variation (COV) equal to 0.1. The COV for t_{ply} is assumed to be 0.01. Specific means and standard deviations are given in Table 2. For completeness, additional numerical analyses have been performed to test the effectiveness of the proposed computational framework, as well as the generality of the ensuing results and conclusions. These tests demonstrated that the framework could be used for any set of random parameters, but the results are not included herein for the sake of brevity.
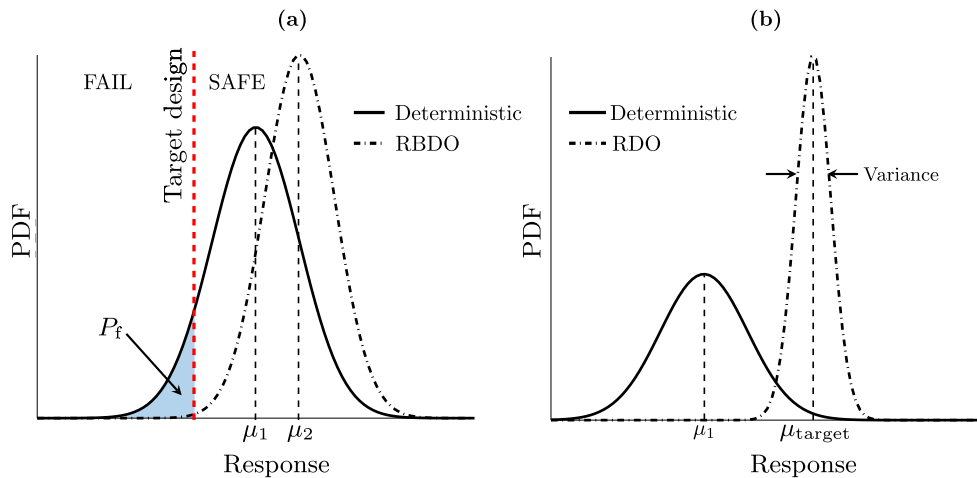

Fig. 5. Changes in the Probability Density Functions of a generic design response due to (a) Reliability-Based Design Optimisation (RBDO) and (b) Robust Design Optimisation (RDO). RBDO minimises P_f, whilst RDO minimises the response variance around a target mean value.

3.2.1. Reliability-based design optimisation (RBDO)

In RBDO, the goal is for a structure to achieve a target performance whilst attaining a prescribed level of design reliability [24]. Reliability is measured in terms of probability of failure, P_f, i.e. constraint violation, or occurrence of a particular response. P_f is calculated as the area between the PDF and the target design constraint as shown in Fig. 5(a).

Aircraft designers aim to minimise aircraft weight subject to stress and other constraints, and aeroelastic tailoring helps to meet this objective. The reliability of the designs can be improved by minimising P_f [23,40], that is by shifting the failure PDF to the right and/or shrinking it. The generalised form of the RBDOs performed in this work is expressed as

$$\begin{aligned}
\underset{\mathbf{x}}{\text{minimize}} \quad & f_{\text{rbdo}}(W(\mathbf{x}, \mathbf{p}), P_f(\mathbf{x}, \mathbf{p})), \\
\text{subject to:} \quad & g_{\text{rc}}(\mathbf{x}, \mathbf{p}) \leqslant 0, \\
& \mathbf{g}_d(\mathbf{x}, \mathbf{p}) \leqslant 0, \\
& \mathbf{x}_L \leqslant \mathbf{x} \leqslant \mathbf{x}_U,
\end{aligned} \tag{14}$$

where f_{rbdo} is the objective function; $g_{\text{rc}}(\mathbf{x})$ is the reliability constraint; $\mathbf{g}_d(\mathbf{x})$ is the vector set of design constraints for which a reliability target is not established; $\mathbf{p}$ is a vector of constant parameters that do not vary in the optimisation; and $\mathbf{x}$ is bound between lower and upper limits, $\mathbf{x}_L$ and $\mathbf{x}_U$.

The objective function is defined as an aggregate of the structural weight and the probability of failure

$$f_{\text{rbdo}} = w_W \times \frac{W}{W_{\text{det}}} + w_{P_f} \times \frac{P_f}{P_{\text{allow}}}, \tag{15}$$

where W_{det} is the structural weight from the deterministic optimisation, and w_W and w_{P_f} are weighting coefficients chosen so that $w_W + w_{P_f} = 1$. Here, the reliability constraint takes the form

$$g_{\text{rc}} = P_f - P_{\text{allow}}, \tag{16}$$

where P_{allow} is the allowable probability of failure. In our case, the probability of exceeding the design flutter speed.

3.2.2. Robust design optimisation (RDO)

RDO aims at optimising a structure placing the targeted performance around a mean value and maximising robustness by minimising sensitivity to random parameter variations [24]. This aim is achieved by minimising the variance and optimising the mean of the response in question, as illustrated in Fig. 5(b). The generalised form of the RDOs performed in this work is

$$\begin{aligned}
\underset{\mathbf{x}}{\text{minimize}} \quad & f_{\text{rdo}}(W(\mathbf{x}, \mathbf{p}), \mu_f(\mathbf{x}, \mathbf{p}), \sigma_f(\mathbf{x}, \mathbf{p})), \\
\text{subject to:} \quad & g_{\text{upper}}(\mu_f(\mathbf{x}, \mathbf{p}), \sigma_f(\mathbf{x}, \mathbf{p})) \leqslant \\
& \quad USL \quad \text{or} \quad g_{\text{lower}}(\mu_f(\mathbf{x}, \mathbf{p}), \sigma_f(\mathbf{x}, \mathbf{p})) \geqslant LSL, \\
& \mathbf{g}_d(\mathbf{x}, \mathbf{p}) \leqslant 0, \\
& \mathbf{x}_L \leqslant \mathbf{x} \leqslant \mathbf{x}_U,
\end{aligned} \tag{17}$$

where f_{rdo} is the objective function defined in terms of weight, weighting coefficients ($\{w_W, w_\mu, w_\sigma\}$: $w_W + w_\mu + w_\sigma = 1$), mean response, μ_f, and standard deviation, σ_f,

$$f_{\text{rdo}} = w_W \times \frac{W}{W_{\text{det}}} + w_\mu \times \left| \frac{\mu_f - \mu_{\text{det}}}{\mu_{\text{det}}} \right| + w_\sigma \times \frac{\sigma_f}{\sigma_{\text{det}}}, \tag{18}$$

and where $g_{\text{upper}} = \mu_f + n\sigma_f$ and $g_{\text{lower}} = \mu_f - n\sigma_f$ are design constraints used to define the solution's robustness. These constraints are bounded by their upper and lower statistical limits, USL and LSL, which are given as functions of the mean and standard deviation of the deterministic optimisation design, μ_{det} and σ_{det}, as

$$USL = \mu_{\text{det}} + n\sigma_{\text{det}} \quad \text{and} \quad LSL = \mu_{\text{det}} - n\sigma_{\text{det}}, \tag{19}$$

entailing that feasibility is maintained within n standard deviations of the optimised mean. In this work, $n = 6$ in line with a 6σ design

philosophy [41].

3.2.3. Robust and reliability design optimisation (RRBDO)

A combined approach, mixing robust and reliability-based design optimisations (RRBDO), is thought to be more comprehensive than RBDO and RDO individually. Particularly when, as in the case of aeroelastic tailoring, design reliability and robustness are sought together. An RRBDO approach is expected to: (a) improve on RDO solutions by bringing additional reliability; and (b) improve on RBDO with increased robustness. In aeroelastic terms, RRBDO should ensure minimum mean weight with mean constrained responses, such as flutter or stresses, all close to the boundary of failure. Mathematically, this is obtained by combining RDO and RBDO constraints as follows:

$$\begin{aligned}
\underset{\mathbf{x}}{\text{minimize}} \quad & f_{\text{rrbdo}}(W(\mathbf{x}, \mathbf{p}), \mu_f(\mathbf{x}, \mathbf{p}), \sigma_f(\mathbf{x}, \mathbf{p})), \\
\text{subject to:} \quad & g_{\text{rc}}(\mathbf{x}, \mathbf{p}) \leq 0, \\
& g_{\text{upper}}(\mu_f(\mathbf{x}, p), \sigma_f(\mathbf{x}, p)) \leqslant \\
& \quad USL \quad \text{or} \quad g_{\text{lower}}(\mu_f(\mathbf{x}, \mathbf{p}), \sigma_f(\mathbf{x}, \mathbf{p})) \geqslant LSL, \\
& \mathbf{g}_d(\mathbf{x}, \mathbf{p}) \leqslant 0, \\
& \mathbf{x}_L \leqslant \mathbf{x} \leqslant \mathbf{x}_U,
\end{aligned} \tag{20}$$

where the objective function, f_{rrbdo}, is

$$f_{\text{rrbdo}} = w_W \frac{W}{W_{\text{det}}} + f_{1,\text{cost}} + f_{2,\text{cost}}, \tag{21}$$

and the cost penalty functions, 5.90 and $f_{2,\text{cost}}$ are defined as

$$f_{1,\text{cost}} = w_\mu \times \left| \frac{\mu_f - \mu_{\text{det}}}{\mu_{\text{det}}} \right| + w_\sigma \times \frac{\sigma_f}{\sigma_{\text{det}}} \quad \text{and} \quad f_{2,\text{cost}} = w_{P_f} \times \frac{P_f}{P_{\text{allow}}}, \tag{22}$$

where w_W, w_μ, w_σ and w_{P_f} are the weighting factors ($\{w_W, w_\mu, w_\sigma, w_{P_f}\}$: $w_W + w_\mu + w_\sigma + w_{P_f} = 1$) and all other quantities retain the meaning defined in §3.2.1 and §3.2.2.

4. Stochastic modelling

For reasons of the computational cost arising from the effects of random parameters variations in optimisation algorithms, sampling methods or stochastic modelling techniques are needed to evaluate model performance quickly. Monte Carlo Simulations [8,19], Polynomial Chaos Expansion [12,16,20,21] and Stochastic Collocation [22] are popular tools for uncertainty quantification. MCSs are simple but require a large number of sample analyses for accurate estimations, which is computationally expensive. Other techniques, such as the perturbation method and PCE, have been introduced to overcome this limitation and provide an alternative to MCS. In the context of aeroelastic tailoring, Castravete & Ibrahim [42] investigated the influence of uncertain bending and torsional stiffness on the flutter behaviour of a wing using both MCSs and a perturbation method. Their results show a good correlation between the two techniques and a computational advantage for the latter. Similar results were presented by [20,12] using PCE.

The method of choice for our work is PCE, which was derived from the Weiner-Askey Chaos Expansion [21,43]. The PCE model for any second-order random process (i.e. any process with finite variance), $u(\theta)$, can be written as

$$\begin{aligned}
u(\theta) = a_0 \Gamma_0 &+ \sum_{i_1=1}^{\infty} a_{i_1} \Gamma_1[\zeta_{i_1}(\theta)] + \sum_{i_1=1}^{\infty} \sum_{i_2=1}^{i_1} a_{i_1 i_2} \Gamma_2[\zeta_{i_1}(\theta), \zeta_{i_2}(\theta)] \\
&+ \sum_{i_1=1}^{\infty} \sum_{i_2=1}^{i_1} \sum_{i_3=1}^{i_2} a_{i_1 i_2 i_3} \Gamma_3[\zeta_{i_1}(\theta), \zeta_{i_2}(\theta), \zeta_{i_3}(\theta)] + \ldots
\end{aligned} \tag{23}$$

where $\Gamma_p[\zeta_{i_1}(\theta), \ldots, \zeta_{i_p}(\theta)]$ is the polynomial chaos of order p in the independent random variables $\{\zeta_{i_1}(\theta), \ldots, \zeta_{i_p}(\theta)\}$, the a terms are

deterministic expansion coefficients and θ is the random character of the quantity involved. The random variables can be modelled using different types of polynomials as described in [12,43]. For example, if $\{\zeta\} = \{\zeta_{i_1}(\theta), ..., \zeta_{i_n}(\theta)\}^T$ is a set of standard Gaussian random variables with zero mean and unit variance, Γ_p can be expressed with n-dimensional Hermite polynomials [43] as

$$\Gamma_p[\zeta_{i_1}(\theta), \, ..., \zeta_{i_n}(\theta)] = (-1)^p e^{\frac{1}{2}\{\zeta\}^T\{\zeta\}} \frac{\partial^p e^{-\frac{1}{2}\{\zeta\}^T\{\zeta\}}}{\partial \zeta_{i_1}(\theta), ..., \partial \zeta_{i_n}(\theta)}. \tag{24}$$

Eq. (23) is often written as

$$u(\theta) = \sum_{i=0}^{\infty} \beta_i \psi_i(\zeta(\theta)), \tag{25}$$

where there is a one-to-one correlation between $\Gamma_p[\zeta_{i_1}(\theta), \, ..., \zeta_{i_p}(\theta)]$ and $\psi_i(\zeta(\theta))$ and between the β and the a terms. For instance, the 2-dimensional expansion of a 3rd order PCE model based on the Gaussian input $\zeta = \{\zeta_1, \zeta_2\}^T$ can be written as (see [20])

$$u_{3rd} = \beta_0 + \beta_1\zeta_1 + \beta_2\zeta_2 + \beta_3(\zeta_1^2-1) + \beta_4\zeta_1\zeta_2 + \beta_5(\zeta_2^2-1) + \beta_6(\zeta_1^3-3\zeta_1)$$
$$+ \beta_7(\zeta_1^2\zeta_2-\zeta_2) + \beta_8(\zeta_2^2\zeta_1-\zeta_1) + \beta_9(\zeta_2^3-3\zeta_2), \tag{26}$$

where the terms β_i are unknown coefficients to be calculated using a computed test data set. In this work, the flutter speed, V_f, is sampled at a series of N points in the design space of the Gaussian material properties. Using Eq. (25), one can write a set of simultaneous equations such that

$$\{V_f\} = [\psi]\{\beta\} + \{\varepsilon\}, \tag{27}$$

where $\{\varepsilon\}$ is the simplification error due to the truncation of expansion. As proposed in [44], a least-squares linear regression model can be used to determine the expansion coefficients. In particular $\{\beta\}$ is found by minimisation of ε such that

$$\varepsilon = \min\left(\sum_{i=1}^{N} \varepsilon_i^2\right), \tag{28}$$

and hence

$$\{\beta\} = (\psi^T\psi)^{-1}\psi^T\{V_f\}. \tag{29}$$

The resulting coefficients are then fed back to Eqn. (27) to emulate the system response for any combination of random variables and to estimate the statistical properties of the system at reduced computational cost.

A general overview of the PCE method is illustrated in Fig. 6. The Latin Hypercube Sampling (LHS) technique [44] is employed to span the sampling space uniformly, so that a relatively small number of samples is sufficient to construct a surrogate model of acceptable fidelity.
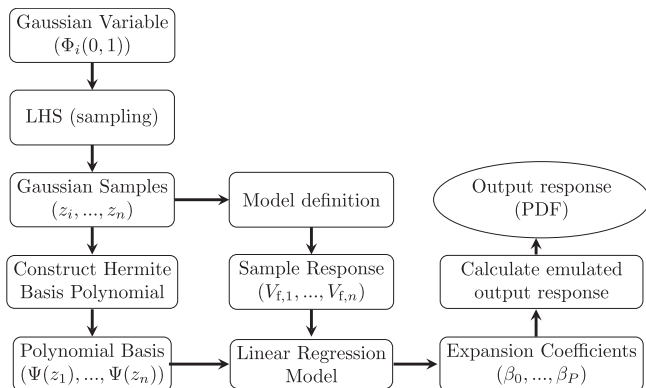

Fig. 6. Overview of the stochastic modelling process using Polynomial Chaos Expansion.

The use of PCE to quantify uncertainty in the optimisation procedure provides a significant reduction in the number of sample runs required in comparison to MCS. A convergence study measuring accuracy of the uncertainty quantification versus the number of samples proves that 30 sample runs are sufficient for the PCE method to converge, which is a 100× less than MCS. The PCE method requires only 6/1000 of the total run time of the MCS. The analysis were conducted on a quad-core Intel Core i7-3770S-CPU @ 3.10 GHz with 8 CPUs and 32 GB RAM. Fig. 7 shows a comparison of the flutter speed distribution obtained from 5000 MCS runs and using PCE models of different order (with random composite material properties as defined in §3.2). An adequate agreement is obtained using 1st, 2nd and 3rd order PCE with 30 samples, with a small discrepancy observed for a 4th order PCE due to an insufficient number of sample runs. These results suggest that sufficiently accurate uncertainty quantifications can be obtained using low order PCE models, i.e. 3rd order, and a small number of sample runs, which contains overall computational cost.

5. Results and discussion

Results obtained using the optimisation framework detailed in previous sections are presented herein, where the benchmark wing model is tailored deterministically as per §3.1 using different combinations of the weighting factors for each of the responses in the cost function. An ideal deterministic optimum is then selected from the Pareto front generated. Subsequently, by following the methods detailed in §3.2, RBDO, RDO and RRBDO are employed to optimise the design for added reliability and/or robustness with minimal structural weight penalty. The effect of uncertainties is quantified for flutter speed and weight. All of the other responses of the deterministic design are kept in the second level optimisation as additional design constraints ($\mathbf{g}_d$) to ensure no deterioration in performance from the first level optimisation.

Henceforth, it is assumed that the random parameters are Gaussian continuous variables. Hermite polynomials are used to construct the polynomial basis in the stochastic model. Thirty LHS sample runs have proven to be sufficient for the analysis.

5.1. Case study I

5.1.1. First level: Deterministic optimisation

A total of 20 optimisation runs is performed, with the weighting factors for each of the responses (as defined in Eq. (11)) assuming values in [0, 1]. These values are chosen using LHS to respect Eq. (12) and are shown in Table 3.

Table 4 presents a summary of the results. In comparison to the benchmark wing, the optimisation reduces structural weight by at least 16.4% (DET9) and up to a maximum of 35.7% (DET8). Interestingly, the lightest solution has a buckling load factor equal to one, suggesting that buckling resistance is critical for minimum weight designs.

Intuitively, cost penalties are incurred when the optimiser is tasked with satisfying multiple constraints. Indeed, the cost function reaches its lowest values for singly constrained optimisations (DET11 to DET14), with the relative reserve factors converging approximatively to the design allowable. A clear example is DET12, for which $w_g = 1$ and $RBM/RBM_{Benchmark}$ is minimum. Similarly, the lowest flutter speed is obtained when $w_f = 1$, i.e. for DET11. Although, it is noted that V_f varies marginally across optimisations, the largest value deviating only 8.1% from $V_{f,Design}$ (DET9).

Further insight into the results can be gained from Fig. 8, where the constraints values of the optimised solutions (for different set of weighting factor) are plotted against the corresponding weighting factor. In theory, the higher the weighting factor, the closer the response should be to its allowable value. This proves to be the case here, which gives confidence into the validity of the underlying calculations.

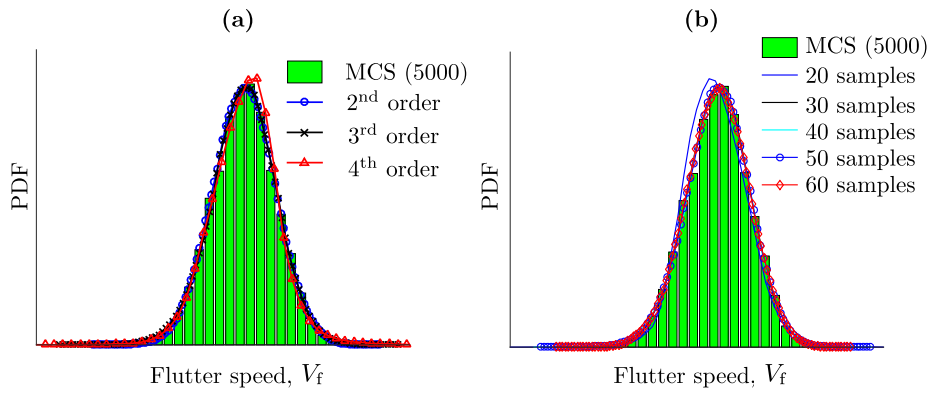The overall best design is derived from the Pareto fronts of Fig. 8, by

Fig. 7. Flutter speed responses obtained using MCS and PCE: (a) MCS and PCE using polynomials of different order; (b) MCS and 3rd order PCE using different number of sample runs.

Table 3
Weighting coefficient values used for deterministic optimisation runs.

Run	Weighting coefficients			
	w_f	w_g	w_{EIG}	w_{FI}
DET1	0.3655	0.3785	0.1164	0.1396
DET2	0.3347	0.2375	0.3102	0.1176
DET3	0.0654	0.3063	0.2832	0.3451
DET4	0.1227	0.2073	0.1127	0.5572
DET5	0.1568	0.7270	0.0804	0.0358
DET6	0.3061	0.4243	0.1713	0.0983
DET7	0.1724	0.1069	0.2595	0.4611
DET8	0.5348	0.0863	0.3324	0.0464
DET9	0.1828	0.1574	0.3638	0.2960
DET10	0.2546	0.4689	0.0721	0.2044
DET11	1.0000	0.0000	0.0000	0.0000
DET12	0.0000	1.0000	0.0000	0.0000
DET13	0.0000	0.0000	1.0000	0.0000
DET14	0.0000	0.0000	0.0000	1.0000
DET15	0.7500	0.1250	0.0625	0.0625
DET16	0.1250	0.7500	0.0625	0.0625
DET17	0.1250	0.1250	0.7500	0.0000
DET18	0.0500	0.3000	0.0500	0.6000
DET19	0.8000	0.1000	0.0500	0.0500
DET20	0.4000	0.4000	0.1000	0.1000

Table 4
Deterministic optimisation results at different weighting factors.

Run	$\dfrac{W}{W_{Benchmark}}$	$\dfrac{V_f}{V_{f,Design}}$	$\dfrac{RBM}{RBM_{Benchmark}}$	λ	FI	$f_{1,cost}$	Σ
DET1	0.669	1.007	0.004	1.006	0.823	0.030	4.974
DET2	0.646	1.001	0.145	1.042	0.601	0.095	45.284
DET3	0.681	1.019	0.032	1.057	0.993	0.030	13.426
DET4	0.676	1.009	0.043	1.022	0.976	0.026	16.486
DET5	0.647	1.007	0.030	1.062	0.859	0.033	12.472
DET6	0.698	1.026	0.026	1.020	0.913	0.031	11.395
DET7	0.683	1.015	0.201	1.029	0.935	0.062	61.986
DET8	0.643	1.001	0.207	1.000	0.589	0.038	63.235
DET9	0.836	1.081	0.180	1.008	0.915	0.071	56.143
DET10	0.654	1.001	0.039	1.029	0.922	0.037	15.195
DET11	0.681	1.000	0.088	1.052	0.725	0.000	29.121
DET12	0.661	1.008	0.003	1.024	0.758	0.003	4.741
DET13	0.709	1.030	0.450	1.001	0.740	0.001	133.535
DET14	0.736	1.048	0.030	1.212	1.000	0.000	12.897
DET15	0.663	1.006	0.321	1.000	0.763	0.060	96.381
DET16	0.772	1.059	0.012	1.095	0.783	0.036	7.646
DET17	0.712	1.036	0.086	1.002	0.860	0.016	28.682
DET18	0.645	1.007	0.037	1.010	1.000	0.012	14.737
DET19	0.646	1.001	0.005	1.408	0.878	0.028	5.778
DET20	0.663	1.006	0.012	1.028	0.952	0.015	7.546

means of the averaging principle defined in Eq. (13). The best design solution is selected from a Pareto point whose give the lowest value for $\Sigma - 5$. DET1 is found to be the Pareto point to be used as the starting point for the second level optimisation. The corresponding wing box sizing parameters are shown is Fig. 9, where they are also compared to the benchmark model. Naturally, thickness values are discontinuous and multiples of t_{ply}. For simplicity, blending constraints were not applied at this stage of the study. However, in order to prevent sharp changes of thickness, no more than two plies were allowed to be dropped between adjacent panels.

5.1.2. Second level: Reliability-based design optimsation (RBDO)

Following on from the first level, DET1 is further optimised for reliability, assuming stochastic variations of material properties (E_1 and G_{12}) and composite ply thickness (t_{ply}). The aleatoric parameters are assumed to have the properties reported in Table 2. The PCE method is used for uncertainty quantification, utilising 30 data samples selected using LHS. Reliability is evaluated in terms of the probability of failure, P_f, of trialled designs to exceed the minimum flutter speed ($V_f/V_{f,Design} > 1$).

The RBDO objective function is formulated in terms of structural weight and probability of failure as indicated by Eq. (15). The allowable probability of failure is set to be equal to the probability of failure of DET1. Hence, $P_{allow} = 8.5 \times 10^{-3}$. Eleven combinations of the weighting factors, w_W and w_{P_f}, are used, as indicated in Table 5.

A design is deemed to be more reliable than the baseline when the probability of failure, or the occurrence of flutter at the design speed, is reduced. To ensure overall design feasibility, first level responses, for which the effect of uncertainties is not evaluated (strain, buckling and gust wing root bending moment), are imposed here as optimisation constraints.

RBDO results are summarised in Table 5. For all combinations of weighting coefficients, the wing box is lighter that the benchmark and the values of P_f are lower than P_{allow}. Except, of course, for RUN 1, for which $w_{P_f} = 0$. The minimum value is obtained for RUN 10, for which $P_f = 2.448 \times 10^{-7}$.

Fig. 10(a) shows that reductions of P_f are due to the flutter PDFs shifting to the right. However, increases in mean flutter speed are accompanied by greater standard deviations, suggesting that reliability is obtained at the expense of robustness. Fig. 10(b) shows the structural weight PDFs resulting from RBDO. It is interesting to note that the distribution of the structural weight obtained for RUN 2 has a lower mean value compared to the deterministic design. This result indicates that it is possible to minimise structural weight whilst improving design reliability. However, all of the other runs have lower probability of failure and higher mean structural weight, demonstrating that a weight penalty is generally necessary for greater reliability.

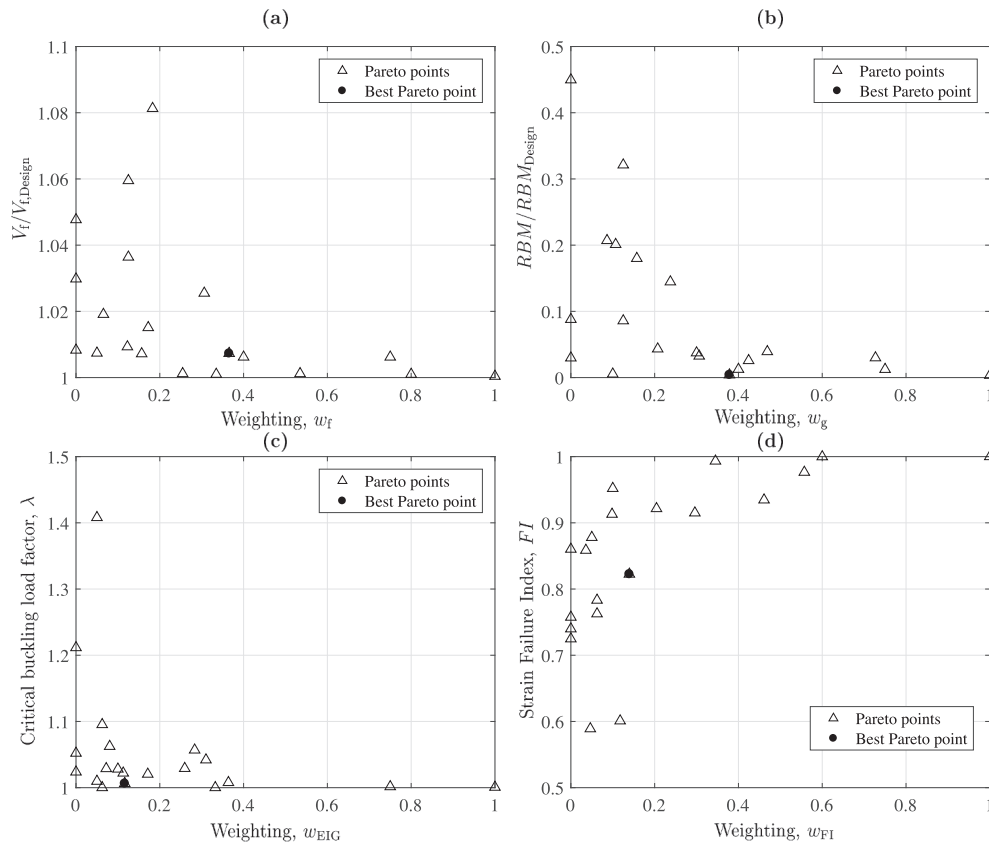The overall best RBDO design is chosen again based on an averaging

Fig. 8. Pareto plots for (a) Flutter constraint against weighting, w_f, (b) RBM constraint against weighting, w_g, (c) Buckling constraint against weighting, w_{EIG} and (d) Strain constraint against weighting, w_{FI}.

principle, in this case, by accounting for the contributions of structural weight and probability of failure at different weighting factor. In particular, the ideal design is picked to be the one having $\Sigma = W/W_{min} + P_f/P_{f,min}$ closest to two. This condition is met by RUN 10 in Table 5, which is 31.8% lighter than the benchmark model and only 1.3% heavier than the best deterministic design.

5.1.3. Second level: Robust design optimisation (RDO)

DET1 is now optimised for robustness following the procedure described in §3.2.2. In particular, we seek a wing box configuration of minimal weight and whose flutter speed distribution, arising from uncertainties in material properties, has mean as close as possible to the deterministic value and minimum standard deviation.

Results are presented in Table 6 and Fig. 11. All design solutions are

characterised by weight reductions in comparison to the benchmark model, mean flutter speeds above the target design value. An increase in robustness is demonstrated by smaller standard deviations in comparison to both DET1 and the RBDO solutions. The minimum reduction from $\sigma_{det} = 2.766$ occurs for RUN 1 ($w_\sigma = 0$) and is 2.6%; the maximum one being 24.9% and occurring for RUN 3 ($w_\sigma = 1$). Having used $V_{f,DET1}$ as an optimisation target, mean flutter speeds cluster uniformly around it. Conversely, all but one RDO solutions have similar or greater weight in comparison to the best deterministic optimum, thus suggesting that an increase in design robustness is likely to be achieved at the expense of weight. Interestingly, some RDO solutions are also sufficiently reliable but these are substantially heavier than their RBDO counterparts.

The overall best RDO design corresponds to RUN 8 and is chosen as the minimiser of $\Sigma - 3$, with $\Sigma = W/W_{min} + \mu_f/\mu_{f,min} + \sigma_f/\sigma_{f,min}$. In
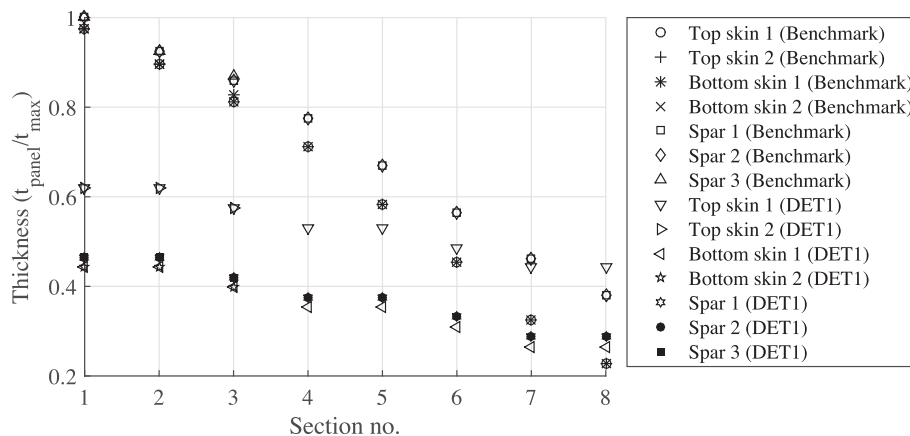

Fig. 9. Thickness variation for skin and spar sections for benchmark and deterministic optimum design (DET1).

Table 5
RBDO solutions obtained using different weighting factors for structural weight and probability of failure.

Run	Weightings		Responses				
ID	w_W	w_{P_f}	$\dfrac{W}{W_{Benchmark}}$	$\dfrac{\mu_f}{V_{f,Design}}$	σ_f	P_f	Σ
1	1.00	0.00	0.669	1.010	2.654	8.500×10^{-3}	34711.896
2	0.90	0.10	0.658	1.013	3.176	2.100×10^{-3}	8576.629
3	0.80	0.20	0.678	1.019	3.684	6.623×10^{-5}	271.485
4	0.70	0.30	0.739	1.026	6.244	4.833×10^{-5}	198.478
5	0.60	0.40	0.689	1.034	5.938	5.001×10^{-6}	21.469
6	0.50	0.50	0.679	1.015	3.046	2.645×10^{-4}	1081.317
7	0.40	0.60	0.729	1.025	5.706	9.974×10^{-6}	41.840
8	0.30	0.70	0.689	1.021	3.805	8.318×10^{-6}	35.016
9	0.20	0.80	0.682	1.023	4.087	2.922×10^{-6}	12.968
10	0.10	0.90	0.682	1.023	3.974	2.448×10^{-7}	2.037
11	0.00	1.00	0.679	1.017	3.451	2.010×10^{-4}	821.843

comparison to the overall best RBDO solution, RUN 8 features lower structural weight and mean flutter speed, and smaller standard deviation.

5.1.4. Second level: Robust and reliability-based design optimisation (RRBDO)

RBDO and RDO results show the following trends: 1) As expected, RBDO solutions tend to be more reliable and less robust than RDO ones, and vice versa; 2) Mean flutter speeds are close to but consistently above the design allowable. With RBDO, these values are also consistently above the mean flutter speed of the overall best deterministic design (DET1). While, with RDO, they are uniformly distributed around it; 3) Reliability or robustness are generally achieved at the expenses of weight, the latter imposing greater penalties. An RRBDO approach is thought to be able to provide a better compromise between weight and design robustness and reliability. Results are presented in Table 7 and Fig. 12.

Notably, most flutter speed PDFs cluster closely, with mean values approximatively 1% above the allowable. Similarly, all runs result in probabilities of failure below P_{allow}. The lowest value is 2.344×10^{-4} which is a 97.2% improvement in comparison to the deterministic design. In terms of robustness, RRBDO results, although generally worse, are comparable with RDO solutions ($\sigma_{f,rdo} \in [2.077, 2.694]$ vs $\sigma_{f,rrbdo} \in [2.555, 2.788]$). A slight increase in minimum structural weight is observed for RRBDO designs in comparison to both RDO and RBDO ones ($W_{rbdo}^{min}/W_{Benchmark} = 0.658$, $W_{rdo}^{min}/W_{Benchmark} = 0.639$, $W_{rbbdo}^{min}/W_{Benchmark} = 0.669$).

Table 6
RDO solutions obtained using different weighting factors for weight, flutter speed mean and standard deviation.

Run	Weightings			Responses			
ID	w_W	w_μ	w_σ	$\dfrac{W}{W_{Benchmark}}$	$\dfrac{\mu_f}{V_{f,Design}}$	σ_f	Σ
1	1.000	0.000	0.000	0.669	1.010	2.694	3.350
2	0.000	1.000	0.000	0.669	1.009	2.668	3.337
3	0.000	0.000	1.000	0.782	1.065	2.077	3.284
4	0.750	0.125	0.125	0.666	1.004	2.564	3.277
5	0.125	0.750	0.125	0.669	1.009	2.598	3.304
6	0.125	0.125	0.750	0.802	1.061	2.088	3.318
7	0.500	0.250	0.250	0.739	1.047	2.564	3.435
8	0.250	0.500	0.250	0.639	1.004	2.352	3.132
9	0.250	0.250	0.500	0.800	1.051	2.570	3.537
10	0.340	0.330	0.330	0.669	1.009	2.632	3.320

The increase in structural weight is thought to be due to the increase in mean flutter speed and the decrease in its standard deviation. These variations are necessary to shift flutter PDFs to the right and to shrink them, which enhances design reliability and robustness. In conclusion, RBBDO results further support the finding that a weight penalty is necessary to impart some level of robustness and reliability to the design. The overall best RBBDO solutions is RUN 7 with a normalised structural weight of 0.679.
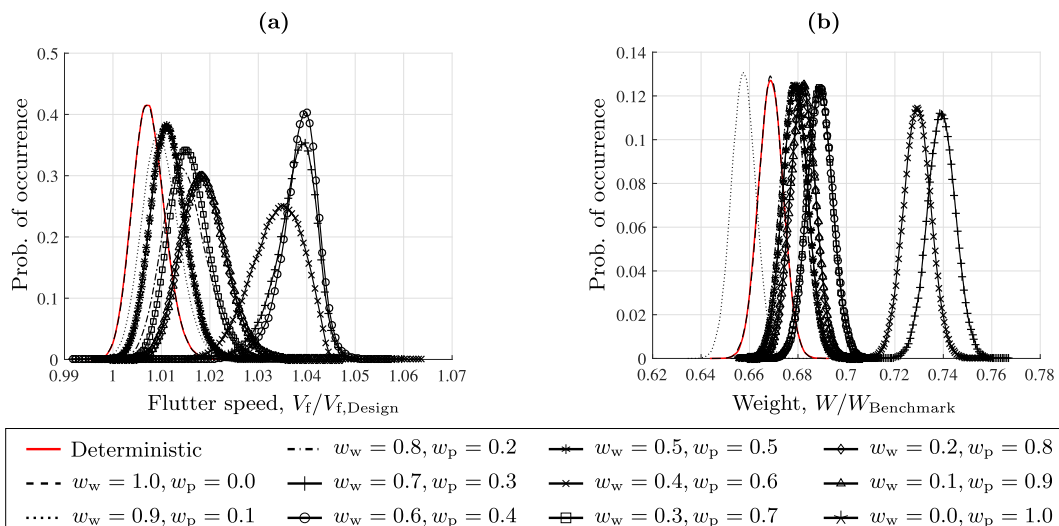

Fig. 10. PDF plots of RBDO solutions for different weighting factors: (a) Flutter speed and (b) Structural weight.
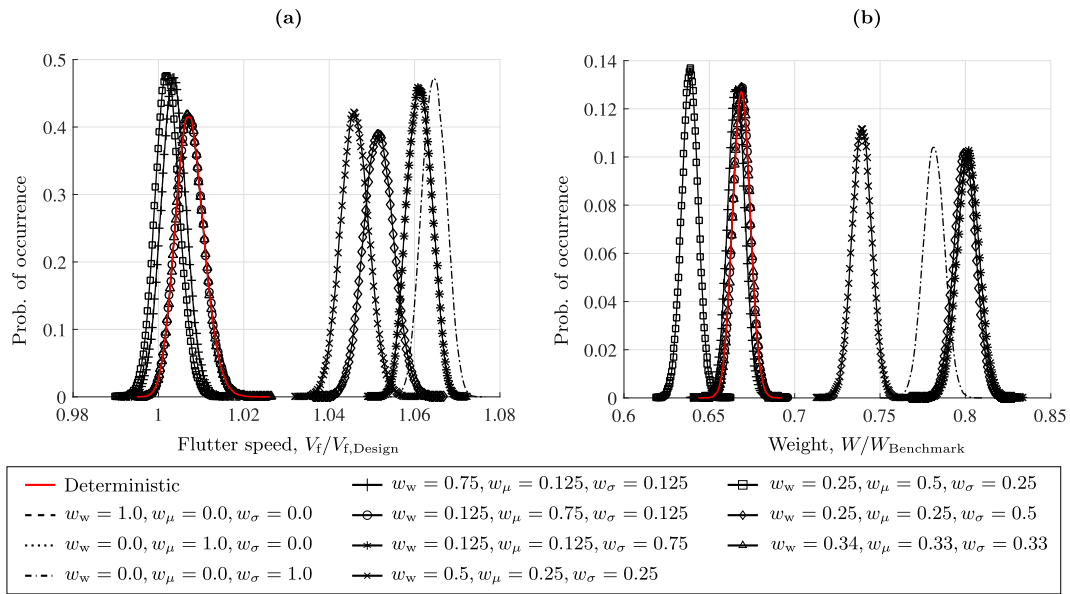
(a)   **(b)**

Fig. 11. PDF plots of RDO solutions: (a) Flutter speed and (b) Structural weight.

Table 7
RRBDO solutions for different weighting values for weight, flutter speed mean and standard deviation, and probability of failure.

| Run	Weighting coefficients				Responses				
ID	w_W	w_μ	w_σ	w_{P_f}	$\dfrac{W}{W_{\text{Benchmark}}}$	$\dfrac{\mu_f}{V_{\text{f,Design}}}$	σ_f	P_f	Σ
1	1.000	0.000	0.000	0.000	0.669	1.011	2.788	8.359×10^{-3}	38.812
2	0.000	1.000	0.000	0.000	0.669	1.010	2.683	7.989×10^{-3}	37.190
3	0.000	0.000	1.000	0.000	0.679	1.015	2.727	2.344×10^{-4}	4.086
4	0.000	0.000	0.000	1.000	0.669	1.010	2.561	8.126×10^{-3}	37.728
5	0.250	0.250	0.250	0.250	0.669	1.010	2.663	8.214×10^{-3}	38.144
6	0.500	0.250	0.125	0.125	0.669	1.010	2.688	8.264×10^{-3}	38.364
7	0.250	0.500	0.125	0.125	0.679	1.014	2.555	2.446×10^{-4}	4.063
8	0.250	0.125	0.125	0.500	0.669	1.010	2.741	8.011×10^{-3}	37.306
9	0.125	0.250	0.500	0.125	0.669	1.010	2.633	7.923×10^{-3}	36.886
10	0.100	0.300	0.300	0.300	0.669	1.009	2.584	7.720×10^{-3}	36.000
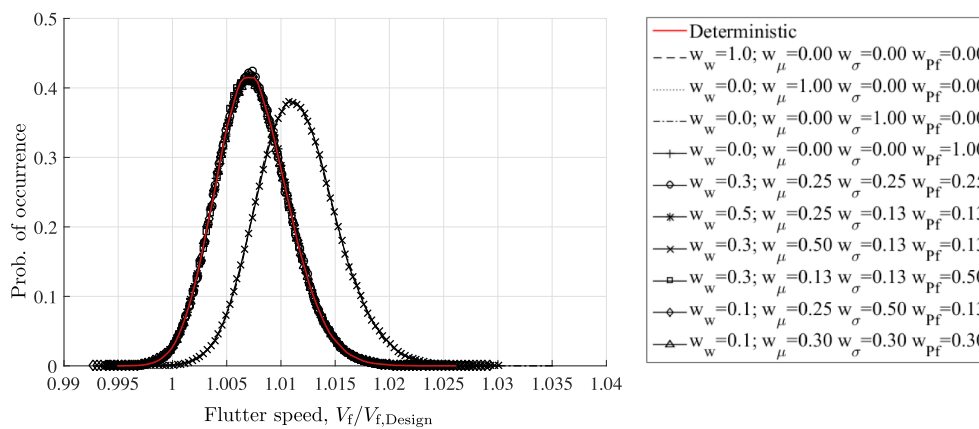
Fig. 12. PDF plots of RRBDO solutions.

6. Conclusions

A multi-level optimisation approach for the robust and/or reliability-based aeroelastic tailoring of a wing box structure is presented. The optimisation objective is to minimise weight subject to multiple constraints, including strength, buckling and flutter margin. The procedure accounts for stochastic variations in input material design parameters. Based on grounds of computational cost, surrogate modelling with Polynomial Chaos Expansion is preferred to Monte Carlo Simulation for the quantification of the effect of uncertainties on structural weight and flutter speed. The results presented in this paper support the following conclusions:

- Polynomial Chaos Expansion is capable of quantifying the effects of uncertainties with sufficient accuracy and fewer model runs in comparison to Monte Carlo Simulations, thus enabling probabilistic design optimisation of a full Finite Element wing box model.
- Reliability-based optimisation shows that reducing the model's probability of failure entails a weight penalty and a loss of design robustness.
- Optimising for robustness successfully reduces the design sensitivity to stocastic variations at the cost of additional weight. Robust designs can also be sufficiently reliable, but generally at a greater weight penalty in comparison to designs optimised for reliability only.
- In general, the model can be optimised for minimal weight and a desired level of reliability or robustness or both. However, enhanced reliability and robustness result in a weight penalty in comparison to the deterministic optimum design.
- Simultaneous robust and reliability-based design optimisation successfully provides the best compromise between weight, reliability and robustness.
- In comparison to the benchmark wing, the framework produces an overall weight reduction of 32.1% for the test case considered, with a 1.5% increase from the first to the second level optimisation to account for stochastic design variations.

Results follow the same pattern when the coefficient of variations of the aleatoric parameters is changed.

Acknowledgements

Appendix A. Supplementary data

Supplementary data associated with this article can be found, in the online version, at https://doi.org/10.1016/j.compstruct.2018.09.086.

References

[1] Eastep F, Tischler VA, Venkayya VB, Khot NS. Aeroelastic tailoring of composite structures. J Aircraft 1999;36(6):1041–7.

[2] Kuzmina S, Chedrik V, Ishmuratov F. Strength and aeroelastic structural optimization of aircraft lifting surfaces using two-level approach. In 6th world congress of structural and multidisciplinary optimization.

[3] Guo S, Li D, Liu Y. Multi-objective optimization of a composite wing subject to strength and aeroelastic constraints. Proc Inst Mech Eng Part G 2011;226(9):1095–106.

[4] Dillinger J, Klimmek T, Abdalla M, Gürdal Z. Stiffness optimization of composite wings with aeroelastic constraints. J Aircraft 2013;50(4):1159–68.

[5] Herencia JE, Weaver PM, Friswell MI. Morphing wing design via aeroelastic tailoring. In 48th AIAA/ASME/ASC Structures, Structural Dynamics & Materials Conference; 2007. pp. 1–19.

[6] Cesnik C, Hodges D, Patil M. Aeroelastic analysis of composite wings. In 37th structure, structural dynamics and materials conference; 1996. 1–11.

[7] Stodieck O, Cooper JE, Weaver PM, Kealy P. Optimization of tow-steered composite wing laminates for aeroelastic tailoring. AIAA J 2015;53(8):2203–15.

[8] Kim T-U, Hwang IH. Optimal design of composite wing subjected to gust loads. Comput Struct 2005;83(19–20):1546–54.

[9] Kim T-U, Shin JW, Hwang IH. Stacking sequence design of a composite wing under a random gust using a genetic algorithm. Comput Struct 2007;85(10):579–85.

[10] Attaran A, Majid DL, Basri S, Mohd Rafie AS, Abdullah EJ. Structural optimization of an aeroelastically tailored composite flat plate made of woven fiberglass/epoxy. Aerosp Sci Technol 2011;15(5):393–401.

[11] Abbas MK, Negm HM, Elshafei MA. Flutter and divergence characteristics of composite plate wing 4(2); 2014: 105–115.

[12] Scarth C, Cooper JE, Weaver PM, Silva GH. Uncertainty quantification of aeroelastic stability of composite plate wings using lamination parameters. Compos Struct 2014;116:84–93.

[13] Guo S, Cheng W, Cui D. Aeroelastic tailoring of composite wing structures by laminate layup optimization. AIAA J 2006;44(12):3146–50.

[14] Kennedy G, Martins J. A comparison of metallic and composite aircraft wings using aerostructural design optimization. In 12th AIAA aviation technology, integration, and operations (ATIO) conference and 14th AIAA/ISSM.

[15] Chang N, Yang W, Wang J, Wang W. Design optimization of composite wing box for flutter and stiffness. In 48th AIAA aerospace sciences meeting including the new horizons forum and aerospace exposition.

[16] Georgiou G, Manan A, Cooper J. Modeling composite wing aeroelastic behavior with uncertain damage severity and material properties. Mech Syst Signal Process 2012;32:32–43.

[17] Gasbarri P, Chiwiacowsky LD, De Campos Velho HF. A hybrid multilevel approach for aeroelastic optimization of composite wing-box. Struct Multidiscip Optim 2009;39(6):607–24.

[18] Melchers RE, Beck AT. Structural reliability analysis and prediction. Wiley; 2018. URL: < https://books.google.co.uk/books?id=8yE6DwAAQBAJ > .

[19] Wiser EP. Monte Carlo technique with correlated random variables 118(2); 1992: 258–272.

[20] Manan A, Cooper J. Uncertainty of composite wing aeroelastic behaviour. In 12th AIAA/ISSMO multidisciplinary analysis and optimization conference.

[21] Xiu D, Em Karniadakis G. Modeling uncertainty in steady state diffusion problems via generalized polynomial chaos. Comput Methods Appl Mech Eng 2002;191(43):4927–48.

[22] Sarkar S, Witteveen JAS, Loeven A, Bijl H. Effect of uncertainty on the bifurcation behavior of pitching airfoil stall flutter. J Fluids Struct 2009;25(2):304–20.

[23] Manan A, Cooper J. Design of composite wings including uncertainties: a probabilistic approach. J Aircraft 2009;46(2):601–7.

[24] Paiva RM, Crawford C, Suleman A. Robust and reliability-based design optimization framework for wing design. AIAA J 2014;52(4):711–24.

[25] Nikbay M, Kuru MN. Reliability based multidisciplinary optimization of aeroelastic systems with structural and aerodynamic uncertainties. J Aircraft 2013;50(3):708–15.

[26] Liang Y, Cheng X-Q, Li Z-N, Xiang J-W. Robust multi-objective wing design optimization via CFD approximation model. Eng Appl Comput Fluid Mech 2011;5(2):286–300.

[27] Marlett K. Hexcel 8552 IM7 Unidirectional Prepreg 190 gsm & 35% RC Qualification Material Property Data Report; 2011. p. 238.

[28] Bloomfield M, Diaconu C, Weaver P. On feasible regions of lamination parameters for lay-up optimization of laminated composites. Proc R Soc A: Math Phys Eng Sci 2009;465(2104):1123–43.

[29] Kameyama M, Fukunaga H. Optimum design of composite plate wings for aeroelastic characteristics using lamination parameters. Comput Struct 2007;85:213–24.

[30] Hahn HT, Tsai SW. Introduction to composite materials. Taylor & Francis; 1980.

[31] Fukunaga H, Sekine H. Stiffness design method of symmetric laminates using lamination parameters. AIAA J 1992;30(11):2791–3.

[32] Grenestedt JL. A study on the effect of bending-twisting coupling on buckling strength. Compos Struct 1989;12(4):271–90.

[33] Johnson EH. MSC Nastran Version 68 Aeroelastic Analysis User's Guide – 2, Structure.

[34] Rao SS. Optimization of airplane wing structures under taxiing loads. Comput Struct 1987;26(3):469–79.

[35] Rao SS, Majumder L. Optimization of aircraft wings for gust loads: interval analysis-based approach. AIAA J 2008;46(3):723–32.

[36] EASA. Certification Specifications for Large Aeroplanes, CS-25 (September); 2008. p. 750.

[37] Poli R, Kennedy J, Blackwell T. Particle swarm optimization. Swarm Intelligence 2007;1(1):33–57.

[38] Hassan R, Cohanim B, de Weck O, Venter G. A comparison of particle swarm optimization and the genetic algorithm. In 46th AIAA/ASME/ASCE/AHS/ASC structures, structural dynamics and materials conference (April); 2005. pp. 1–13.

[39] Mourelatos ZP, Liang J. A methodology for trading-off performance and robustness under uncertainty. J Mech Des 2006;128:856.

[40] C. Scarth, P. Sartor, J. Cooper, Robust Aeroelastic Design of Composite Plate Wings, 17th AIAA Non-Deterministic Approaches Conference (January) (2015) 1–13.

[41] Park GJ, Lee TH, Lee KH, Hwang K-H. Robust design: an overview. AIAA J 2006;44(1):181–91.

[42] Castravete SC, Ibrahim RA. Effect of stiffness uncertainties on the flutter of a cantilever wing. AIAA J 2008;46(4):925–35.

[43] Xiu D, Karniadakis GE. The Wiener-Askey polynomial chaos for stochastic differential equations. SIAM J Scientific Comput 2002;24(2):619–44.

[44] Choi S-K, Grandhi RV, Canfield RA, Pettit CL. Polynomial chaos expansion with latin hypercube sampling for estimating response variability. AIAA J 2004;42(6):1191–8.